

Propagation of ultra-high energy neutrinos in the cosmic neutrino background

V. Van Elewyck^{a*}

^aInstitut de Physique Nucléaire d'Orsay
15, rue G. Clémenceau, 91406 Orsay Cedex, France
Email: vero@ipno.in2p3.fr

UHE cosmic neutrino interaction with the cosmic neutrino background (CnuB) is expected to produce absorption dips in the UHE neutrino flux at energies above the threshold for Z-boson resonant production. The observation of these dips would constitute an evidence for the existence of the CnuB; they could also be used to determine the value of the relic neutrino masses as well as some features of the population of UHE neutrino sources. After briefly discussing the current prospects for relic neutrino spectroscopy, we present a calculation of the UHE neutrino transmission probability based on finite-temperature field theory which takes into account the thermal motion of the relic neutrinos. We then compare our results with the approximate expressions existing in the literature and discuss the influence of thermal effects on the absorption dips in the context of realistic UHE neutrino fluxes and favoured neutrino mass schemes.

1. Introduction and motivations

The existence of a cosmological background of relic neutrinos (CνB), characterized by a present temperature of $T_{\nu 0} \approx 1.95$ K (1.69×10^{-4} eV) and a number density $n_{\nu 0} \approx 56$ cm⁻³ per species, is a robust prediction of Big Bang cosmology [1]. Its presence, at least at early times, seems now confirmed by data coming from observational cosmology, which also provide bounds on the number of neutrino species (now greater than zero) and on their absolute mass scale (see [2] for an extensive discussion of these issues). Direct detection of the CνB at present time is however much more problematic. Several laboratory experiments (discussed i.e. in [3]) have been proposed to detect relic neutrino through their weak interactions, using torsion balances or even accelerated beams of nuclei, but the technological improvements required in those experimental setups are way beyond the state of the art.

An interesting alternative is provided by exploiting cosmic rays - actually ultra-high energy cosmic neutrinos (UHEν) - as a natural beam and search for evidence of their interaction with the

relic neutrino background. Two approaches have emerged in that context: the first one searches for "emission" features and the production of charged cosmic rays or photons beyond the GZK cutoff, through the so-called "Z-burst" mechanism [4,5] (the dominant UHEν- CνB interaction channel being $\nu \bar{\nu} \rightarrow Z \rightarrow X$). This mechanism probes the universe delimited by the GZK sphere and is therefore sensitive to local overdensities in the CνB that may arise from the gravitational clustering on massive structures, like the Virgo cluster [6], and would result in a directional excess of UHE cosmic rays.

The second approach, on which we will concentrate here, looks for "absorption" features in the UHEν flux that would reflect their interaction with the relic neutrinos along their path [7,8,9,10,11]. As illustrated below, the position of the absorption dip approximately corresponds to the redshifted resonance energy for the Z-boson exchange, namely

$$K_{res} \approx \frac{M_Z^2}{2m_\nu(1+z_s)} \quad (1)$$

so that it directly depends on the value of the neutrino mass m_ν and of the source redshift z_s . The shape and depth of the dip also reflect to some

*supported by CNRS-IN2P3 and the European Community under Marie Curie Fellowship MEIF-CT-2005 025057.

extent the neutrino mixing pattern as well as the characteristics and distribution of UHE ν sources. In that sense, and provided adequate sensitivity and energy resolution of the detectors, a detailed spectroscopic study of the UHE ν flux could allow the determination of the absolute neutrino masses along with an experimental proof of existence of the C ν B [12,13]. This mechanism has generated a renewed interest in the light of the recent results obtained both in observational cosmology and for determination of the neutrino mass and mixing schemes.

However, most of the work in the literature describe the UHE ν -C ν B interactions assuming that relic neutrinos are at rest, while the effects of thermal motion should be included as soon as the momentum of relic neutrinos becomes comparable to their mass (or even before). Therefore we have chosen to address the question of relic neutrino spectroscopy in the framework of finite-temperature field theory (FTFT), which allows to take into account the thermal effects in a systematic way [17]. In section 2, we briefly present our calculation of the damping of an UHE neutrino travelling across the C ν B and determine the absorption probability for a neutrino emitted at a given redshift. We then illustrate our calculations in two realistic contexts and explore various combinations of parameters to investigate the differences between the FTFT calculation and previous approximations. In section 3 we discuss how the thermal broadening of the absorption lines in the UHE ν flux could affect the determination of m_ν and of the characteristics of the UHE ν source population. In section 3 we comment our results in the context of relic neutrino clustering, for different hypothesis on the density and scale of the clusters. Concluding remarks are presented in section 5.

2. Damping of UHE neutrinos across the relic neutrino background

The equation of motion of an UHE neutrino with four-momentum $k^\mu = (\mathcal{E}_K, \vec{K})$ and mass m_ν traveling across the C ν B reads

$$(k - m_\nu - \Sigma)\psi = 0 \quad (2)$$

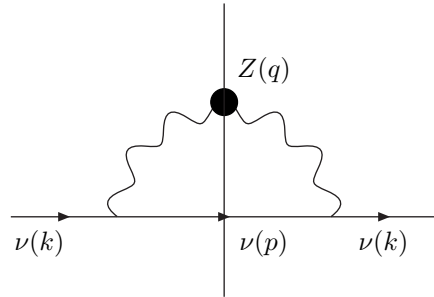


Figure 1. Feynman diagram for the one-loop self-energy of an UHE neutrino due to a Z-boson exchange with an (anti-)neutrino from the relic background; the blob on the Z propagator indicates that we use the dressed propagator and the cut is to select the imaginary part of the diagram.

where the self-energy Σ accounts for the interactions with the surrounding medium. The dominant process is here the Z-boson exchange in the s-channel, as shown in fig. 1. We determine Σ from a FTFT one-loop calculation carried out in terms of the (vacuum) Z propagator and the thermal propagator of the relic neutrinos. The latter depends on the functions $f_\nu(P)$ and $f_{\bar{\nu}}(P)$ which describe the momentum distributions of neutrinos (antineutrinos) in the thermal bath. These functions take the simple relativistic Fermi-Dirac form

$$f_\nu(P) = f_{\bar{\nu}}(P) = \frac{1}{(e^{P/T_\nu} + 1)}, \quad (3)$$

where T_ν is the temperature of the C ν B and we have neglected the chemical potential. It is worth noting here that, although relic neutrinos are not relativistic anymore at present time, their distribution has maintained the form it had at the time of neutrino decoupling, corresponding to $T_\nu \sim 1$ MeV.

The dispersion relation corresponding to eq. (2) is given by $\mathcal{E}_K = \mathcal{E}_r(K) - i\gamma(K)/2$, where \mathcal{E}_K and γ are functions of K . The damping factor γ governs the propagation of the UHE ν across the background of relic neutrinos and is directly related to the imaginary part of the self-energy,

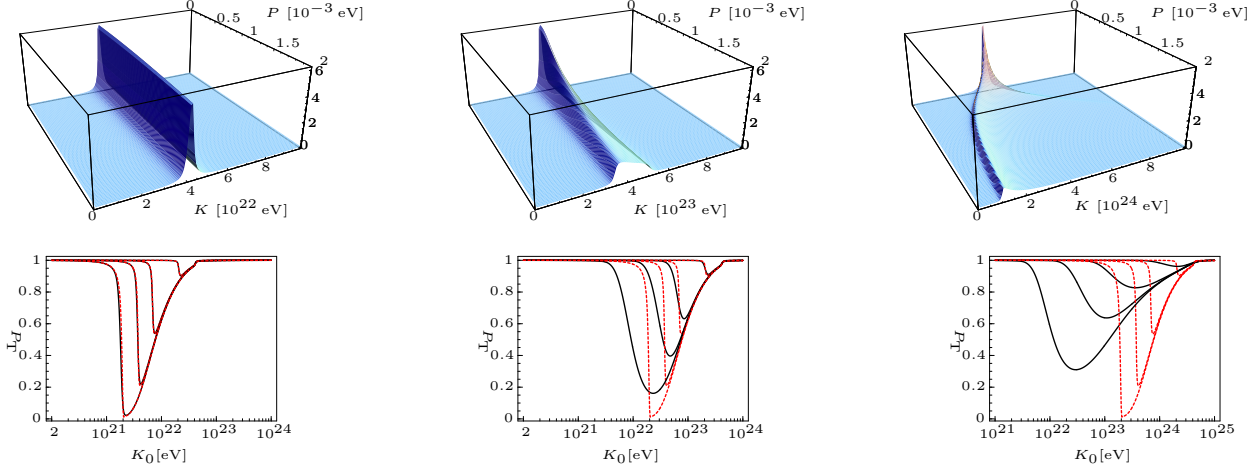


Figure 2. **Top** : cross-section $\sigma_{\nu\bar{\nu}}(P, K)$, in units of 10^{-31} cm^2 , as given by eq. (6), as a function of the energy of the incident neutrino, K , and of the relic neutrino momentum, P . From left to right, the panels correspond to a neutrino mass 10^{-1} , 10^{-2} , and 10^{-3} eV. **Bottom** : Transmission probability $P_T(K_0, z_s)$ as a function of the UHE ν energy as detected on Earth, K_0 , for a source located at redshifts $z_s = 1, 5, 10, 20$ (from top to bottom in each panel) and for a neutrino mass $m_\nu = 10^{-1}, 10^{-2}, 10^{-3}$ eV (from left to right). The continued, black curves correspond to the full damping as given by eqs. (5) and (6), while the dotted (red) curves are for the approximation of relic neutrinos at rest, eq.(7).

Σ_i [16]. In the approximation that the UHE ν are ultrarelativistic and that we can neglect the background effects on their energy ($\mathcal{E}_r(K) \simeq K$), the damping can be written as (see [17] for the detailed calculation)

$$\gamma_{\nu\bar{\nu}}(K) = -\frac{1}{K} \text{Tr}(k\Sigma_i)|_{\mathcal{E}_r=K} \quad (4)$$

$$= \int_0^\infty \frac{dP}{2\pi^2} P^2 f_{\bar{\nu}}(P) \sigma_{\nu\bar{\nu}}(P, K). \quad (5)$$

For $m_\nu \ll M_Z, K$ and neglecting terms of order Γ_Z^2/M_Z^2 , we have

$$\begin{aligned} \sigma_{\nu\bar{\nu}}(P, K) &= \frac{2\sqrt{2}G_F\Gamma_Z M_Z}{2KE_p} \left\{ 1 + \frac{M_Z^2}{4KP} \right. \\ &\times \ln \left(\frac{4K^2(E_p + P)^2 - 4M_Z^2 K(E_p + P) + M_Z^4}{4K^2(E_p - P)^2 - 4M_Z^2 K(E_p - P) + M_Z^4} \right) \\ &+ \frac{M_Z^3}{4K P \Gamma_Z} \left[\arctan \left(\frac{2K(E_p + P) - M_Z^2}{\Gamma M_Z} \right) \right. \\ &\left. \left. - \arctan \left(\frac{2K(E_p - P) - M_Z^2}{\Gamma M_Z} \right) \right] \right\}. \quad (6) \end{aligned}$$

where $E_p = \sqrt{P^2 + m_\nu^2}$ is the energy of the relic neutrino. Taking the limit of eq. (6) for

$P \rightarrow 0$, one recovers the approximated cross-section used for relic neutrinos at rest, with the Z peak at the UHE ν "bare" resonance energy $K_{res} = M_Z^2/(2m_\nu)$. The damping reads in that case

$$\begin{aligned} \gamma_{\nu\bar{\nu}}^0(K) &= 2\sqrt{2}G_F\Gamma_Z M_Z n_\nu \\ &\times \frac{2Km}{4K^2 m^2 - 4M_Z^2 Km + M_Z^4}, \quad (7) \end{aligned}$$

in agreement with the results of [8]. The expressions used in [10] can be obtained by further evaluating the cross-section at the pole of the resonance, $2mK_{res} = M_Z^2$ (narrow-width approximation). However, this approximation is no longer valid for relatively small m_ν and/or large C ν B temperatures: fig. 1 (top line) shows how the resonance peak in the $\nu\bar{\nu} \rightarrow Z$ cross-section broadens and shifts to lower UHE ν energies as P increases. Actually two effects combine: the modification of the cross-section peak due to its dependance in E_p , and the thermal distribution which selects a range of relic neutrino momenta close to the temperature of the C ν B. The net effect of this thermal broadening is a reduction of the damping, which affects the transmission prob-

ability and the depth and shape of the absorption dips.

The transmission probability for an UHE ν emitted at a redshift z_s to be detected on Earth with an energy K_0 is obtained by integrating the damping along the UHE ν path, taking into account that both the UHE ν energy and the C ν B temperature are redshifted:

$$P_T(K_0, z_s) = \exp \left[- \int_0^{z_s} \frac{dz}{H(z)(1+z)} \gamma_{\nu\bar{\nu}}(K_0(1+z)) \right], \quad (8)$$

where $H = H_0 \sqrt{0.3(1+z)^3 + 0.7}$ is the Hubble factor as suggested by recent observations [14]. Fig. 1 (bottom line) compares the transmission probabilities obtained from eqs. (5) and (7), for an UHE ν emitted at different redshifts and m_ν ranging from 10^{-1} to 10^{-3} eV. As long as $m_\nu/T_\nu \geq 10^{-2}$, the shape of the absorption dip is not affected by thermal broadening and is rather sharply delimited, at high energies, by the bare resonant energy for the propagating neutrino, $K_0 = K_{res} = M_Z^2/(2m_\nu)$, and at low energies by the redshifted resonant energy $K_0 = K_{res}/(1+z_s)$. Evaluating the position of these points would in principle allow us to determine m_ν as well as z_s , the redshift at which the UHE ν was emitted. As m_ν/T_ν decreases, however, the absorption dips get broadened and shift to lower energies, and this effect also increases with the redshift since UHE neutrinos from distant sources are emitted in a hotter background.

3. Absorption lines in the UHE neutrino flux

The results presented so far deal with a monoenergetic source of UHE ν located at a given redshift. A realistic situation would more probably involve a distribution of sources which emit UHE ν with some given energy spectrum and flavor composition, the latter evolving along the neutrino pathway. To investigate these effects, and following the approach of [10], we have considered a flux of UHE ν of the form:

$$\mathcal{F}_\nu(K_0) = \frac{1}{4\pi} \int_0^\infty \frac{dz}{H(z)} P_T(K_0, z) \eta(z) J_\nu(K_0).so$$

The distribution of sources,

$$\eta(z) = \eta_0 (1+z)^n \theta(z - z_{\min}) \theta(z_{\max} - z), \quad (9)$$

is well-suited for an approximate description of models ranging from astrophysical production sites ("bottom-up" mechanisms for which $n \simeq 4$ and $z_{\max} \leq 10$) to exotic, non-accelerator sources (which typically have $n \simeq 1-2$ and may extend to larger redshifts). The injection spectrum is taken as a power-law with a cutoff at some high energy $K_{\max} > K_{res}(1+z)$ (we do not consider here the possibility of broken power-law spectra):

$$J_\nu(K) = j_\nu K^{-\alpha} \theta(K_{\max} - K) \quad (10)$$

with the spectral index α ranging between 1 and 2, depending on the production mechanism considered. Under these assumptions, the normalized flux only depends on the difference $n - \alpha$ of the spectral indexes. We then computed numerically the UHE ν flux produced for two distinct values of the spectral index combination: $n - \alpha = 2$, which is representative of a distribution of astrophysical sources, and $n - \alpha = 0$, which could describe the UHE ν flux produced through some top-down process.

As for the flavor content of \mathcal{F}_ν , the ratio predicted for standard, hadronic sources is $J_{\nu_e} : J_{\nu_\mu} : J_{\nu_\tau} = 1 : 2 : 0$, while more exotic mechanisms could be characterized by a democratic $J_{\nu_e} : J_{\nu_\mu} : J_{\nu_\tau} = 1 : 1 : 1$. In both cases, and in view of our current knowledge of the neutrino mixing parameters, it is reasonable to think that the total neutrino flux detected at Earth will just be the sum on all three neutrino mass eigenstates [10]. Therefore we considered mass patterns compatibles with the favoured 3-neutrino hierarchical schemes [15], namely:

$$\begin{aligned} normal : & \quad m_3 = 5 \cdot 10^{-2} \text{ eV}, \quad m_2 = 9 \cdot 10^{-3} \text{ eV} \\ inverted : & \quad m_3 = m_2 = 5 \cdot 10^{-2} \text{ eV} \end{aligned}$$

and chose the values $m_1 = 10^{-3}$ eV or 10^{-4} eV for the third, unknown mass.

The results are presented in figs. 3 and 4, which display the all-flavour UHE ν flux as a function of the present energy K_0 of the UHE neutrino, normalized to the flux in absence of absorption effects. Both figures show how thermal broadening globally modify the shape and extension of the

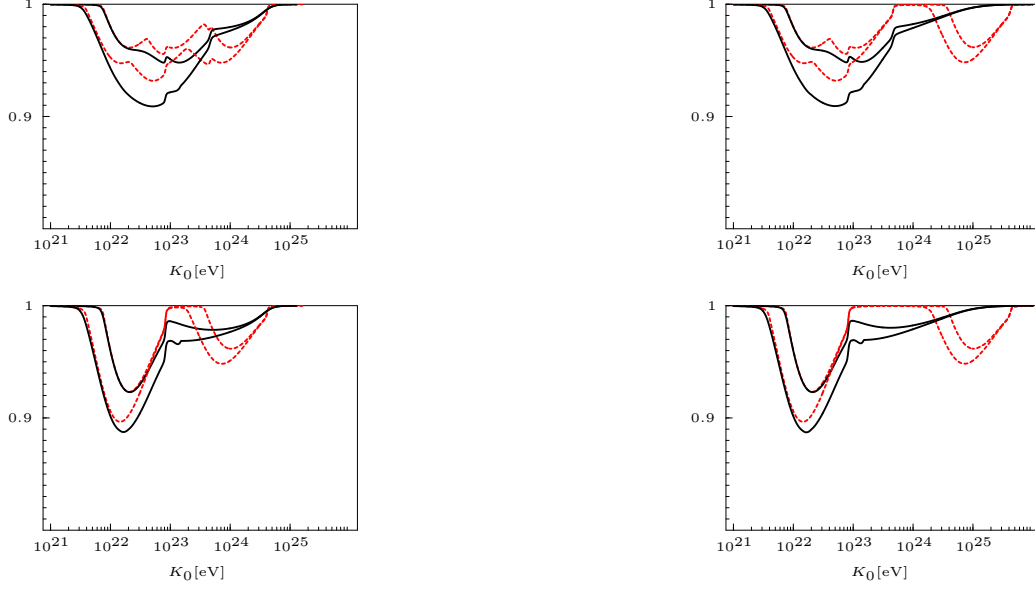


Figure 3. UHE ν flux in presence of damping, \mathcal{F}_ν , with $\alpha - n = 0$ and $z_s = 10, 20$ (typical top-down model), normalized to the corresponding flux in absence of interactions. The top row is for the normal neutrino mass hierarchy and the bottom one for the inverted hierarchy. Plots on the left have $m_1 = 10^{-3}$ eV and plots on the right $m_1 = 10^{-4}$ eV. Colour code is as in fig. 1.

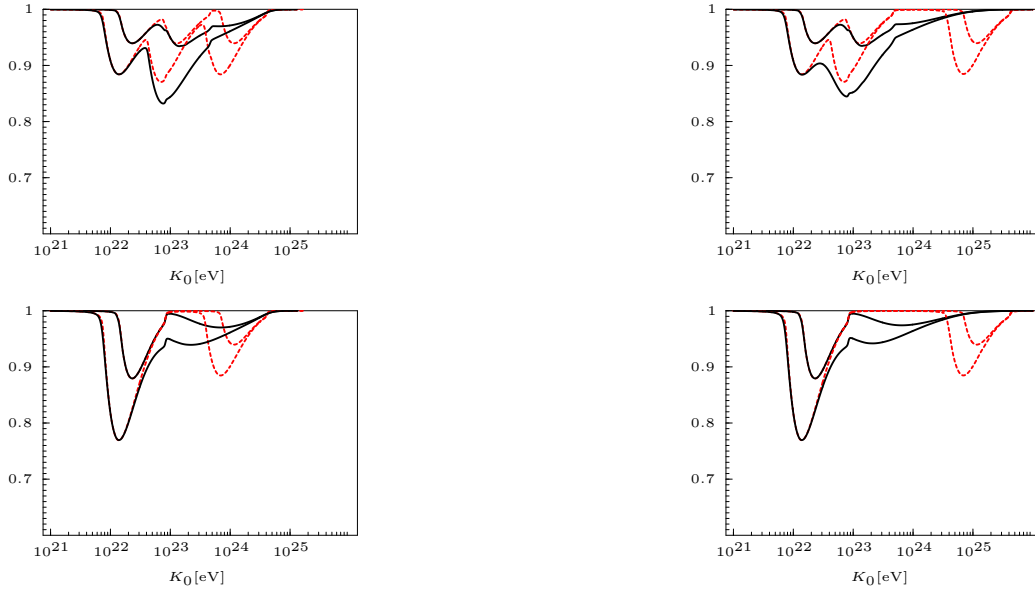


Figure 4. UHE ν flux in presence of damping, \mathcal{F}_ν , with $\alpha - n = 2$ and $z_s = 5, 10$ (typical bottom-up model), normalized to the corresponding flux in absence of interactions. The top row is for the normal neutrino mass hierarchy and the bottom one for the inverted hierarchy. Plots on the left have $m_1 = 10^{-3}$ eV and plots on the right $m_1 = 10^{-4}$ eV. Colour code is as in fig. 1.

absorption lines respect to the approximated case. The dip corresponding to the smallest mass is almost always washed out and only contribute to further broadening the line at high energies. For very large z_{max} , the merging of the two other dips in the normal hierarchy scheme makes it more difficult to differentiate from the inverted one.

4. Absorption lines in the case of relic neutrino clustering

The possible clustering of relic neutrinos onto dark matter halos has been intensively studied, in particular in the context of the generation of the UHE cosmic rays through the Z-burst mechanism [4,5]. Recent calculations using Vlasov (Boltzmann collisionless) equation have presented revised estimations of the density profiles and typical spatial extension of the neutrino clusters [18,19]. They give overdensities of the order of $10\text{-}10^4 n_{0\nu}$ and cluster scales $L \sim 0.01 - 1$ Mpc, depending on the neutrino mass, the mass of the attracting halo and its velocity dispersion (typically 200 km/s for a galaxy and 1000 km/s for a galaxy cluster). Limits to the clustering of neutrinos on large scales are also set by the Pauli exclusion principle and the limit on the maximum phase-space density [20], which imply that only neutrinos with mass $m_\nu \geq 1$ eV will efficiently cluster on galactic halos ($L_G \sim 50$ kpc), while neutrinos with $m_\nu \geq 0.1$ eV can cluster on the much bigger scales associated to halos of (super-)clusters ($L_C \sim 1$ Mpc) [5,18,19].

To compute the UHE ν absorption due to clustered neutrinos, we substituted $f_\nu(P)$ in eq.(5) by a modified Fermi-Dirac distribution,

$$f_\nu^{\text{cl}}(P) = \frac{1}{2} \frac{e^{-\Phi/T_\nu} + 1}{e^{(P-\Phi)/T_\nu} + 1}. \quad (11)$$

which parametrises reasonably well the distributions functions presented in [19] in function of a single parameter Φ . The neutrino density corresponding to eq.11 is

$$n_\nu^{\text{cl}} = -\frac{T_\nu^3}{2\pi^2} (1 + e^{-\Phi/T_\nu}) \text{Li}_3(-e^{\Phi/T_\nu}), \quad (12)$$

where $\text{Li}_3(x)$ is the trilogarithm function. We also

assume that the cluster density is constant, i.e.

$$\begin{cases} n_\nu = N_{\text{cl}} n_{\nu 0} & r < L_{\text{cl}} \\ n_\nu = n_{\nu 0} & r > L_{\text{cl}}, \end{cases}$$

so that $f_\nu(P)$ does not depend on the position. For a given overdensity factor N_{cl} we then solve $n_\nu^{\text{cl}} = N_{\text{cl}} n_{\nu 0}$ numerically for Φ .

We then computed the transmission probability for a cluster of relic neutrinos with mass 0.1 or 1 eV, located between the UHE ν source and the observer. As expected, the effect of the thermal motion of the neutrinos is generally negligible or small due to the relatively small overdensities achievable and the absence of redshift effect in T_ν . Fig. 5 shows that we have to saturate the bounds on both parameters N^{cl} and L_{cl} to obtain a significant effect on the depth of the absorption line: for a maximal overdensity factor $N_{\text{cl}} = 10^4$, the maximum absorption probability across the cluster is reduced from $\approx 55\%$ to $\approx 35\%$.

5. Conclusions

The study of both absorption and emission features in the spectrum of UHE neutrinos offers probably today's most promising method for a relatively direct observation of the cosmic neutrino background. This is especially true in view of the upcoming generation of detectors, like ICECUBE [21], ANITA [22], FORTE [23], GLUE [24], the Pierre Auger Observatory [25],... which are already putting limits on the UHE ν flux and starting to constrain the corresponding theoretical models.

One has however to keep in mind that the thermal motion of the the relic neutrinos could significantly affect the shape and position of the absorption dips in the UHE ν spectrum. From the exploration of the parameter space currently allowed by astrophysical and cosmological constraints, we have seen that, even in the regime of non-relativistic neutrinos, the dips can be broadened and shifted to lower energies. This will complicate their observation in real experiments, especially if the UHE ν source population is concentrated at small redshifts, producing rather shallow and extended dips. The shift to lower energies, where neutrino fluxes are expected to be

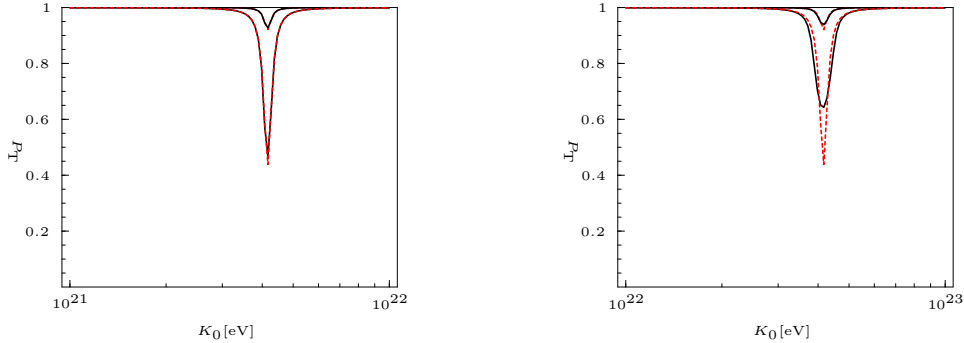


Figure 5. Transmission probability for a cluster of extension 1 Mpc, made of neutrinos of mass 1 eV (left) and 10^{-1} eV (right), with a constant neutrino density $n_{\nu}^{\text{cl}} = 10^3 n_{0\nu}$ and $n_{\nu}^{\text{cl}} = 10^4 n_{0\nu}$ (from top to bottom in each plot). The colour code is the same as in fig. 1.

higher, could in principle increase the detection potential respect to the case of a relic neutrino at rest with the same mass. Still, the situation will be more intricate if the pattern of neutrino mass eigenstates is such that their combined effect results in a superposition of dips with different depths and extensions. Considering the small number of events expected in the UHE ν detectors at those high energies, it seems rather unrealistic to resolve the detail of these complex absorption patterns.

As for the case of UHE ν going through relic neutrino clusters, we have seen that the effect on the absorption is relatively small compared to that of UHE ν that travel on cosmological distances, since clustering only occurs at small redshifts. For the same reason, and because only rather heavy neutrinos do cluster, thermal effects have a limited impact on the shape of the absorption lines and only result in their attenuation. On the other hand, nearby clusters of relic neutrinos are expected to play an important role in the context of the Z-burst mechanism and the emission of UHE cosmic rays.

REFERENCES

1. P. J. E. Peebles, *Principles of Physical Cosmology*, Princeton University Press, 1993; E.W. Kolb and M.S. Turner, *The Early Universe*, Addison-Wesley, Redwood City, 1990.
2. S. Hannestad, *New J. Phys.* **6** (2004) 108 [arXiv:hep-ph/0404239]; J. Lesgourgues and S. Pastor, *Phys. Rept.* **429**, 307 (2006) [arXiv:astro-ph/0603494].
3. B. Eberle, “*Big bang relic neutrinos and their detection*”, DESY-THESIS-2005-024
4. D. Fargion, B. Mele, and A. Salis, *Astrophys. J.* **517**, 725 (1999) [arXiv:astro-ph/9710029].
5. T. J. Weiler, *Astropart. Phys.* **11**, 303 (1999) [arXiv:hep-ph/9710431].
6. A. Ringwald, T. J. Weiler, and Y. Y. Y. Wong, arXiv:astro-ph/0505563.
7. T. J. Weiler, *Phys. Rev. Lett.* **49**, 234 (1982) and *Astrophys. J.* **285**, 495 (1984).
8. E. Roulet, *Phys. Rev. D* **47**, 5247 (1993).
9. S. Yoshida, *Astropart. Phys.* **2** (1994) 187; S. Yoshida, H. y. Dai, C. C. H. Jui, and P. Sommers, *Astrophys. J.* **479**, 547 (1997)
10. B. Eberle, A. Ringwald, L. Song, and T. J. Weiler, *Phys. Rev. D* **70**, 023007 (2004).
11. G. Barenboim, O. Mena Requejo, and C. Quigg, *Phys. Rev. D* **71** (2005) 083002.
12. H. Pas and T. J. Weiler, *Phys. Rev. D* **63** (2001) 113015.
13. D. Fargion, P. G. De Sanctis Lucentini, M. Grossi, M. De Santis, and B. Mele, *Mem. Soc. Ast. It.* **73** (2002) 848.
14. D. N. Spergel *et al.* [WMAP Collaboration], *Astrophys. J. Suppl.* **148** (2003) 175

- [arXiv:astro-ph/0302209].
15. J. F. Beacom and N. F. Bell, Phys. Rev. D **65** (2002) 113009.
 16. J. C. D’Olivo and J. F. Nieves, Phys. Rev. D **52** (1995) 2987.
 17. J. C. D’Olivo, L. Nellen, S. Sahu and V. Van Elewyck, Astropart. Phys. **25** (2006) 47 [arXiv:astro-ph/0507333].
 18. S. Singh and C. P. Ma, Phys. Rev. D **67**, 023506 (2003) [arXiv:astro-ph/0208419].
 19. A. Ringwald and Y. Y. Y. Wong, JCAP **0412**, 005 (2004) [arXiv:hep-ph/0408241].
 20. S. Tremaine and J. E. Gunn, Phys. Rev. Lett. **42** (1979) 407.
 21. J. Ahrens *et al.* [The IceCube Collaboration], Nucl. Phys. Proc. Suppl. **118** (2003) 388.
 22. S. W. Barwick *et al.* [ANITA Collaboration], Phys. Rev. Lett. **96** (2006) 171101.
 23. N. G. Lehtinen, P. W. Gorham, A. R. Jacobson and R. A. Roussel-Dupre, Phys. Rev. D **69** (2004) 013008.
 24. P. W. Gorham, C. L. Hebert, K. M. Liewer, C. J. Naudet, D. Saltzberg and D. Williams, Phys. Rev. Lett. **93** (2004) 041101
 25. X. Bertou, P. Billoir, O. Deligny, C. Lachaud and A. Letessier-Selvon, Astropart. Phys. **17** (2002) 183.